Inorganic Materials, Vol. 41, No. 3, 2005, pp. 255–260. Translated from Neorganicheskie Materialy, Vol. 41, No. 3, 2005, pp. 314–320.

Structure of Amorphous Alumina Tubes Studied by Positron Annihilation Lifetime Spectroscopy

V. P. Shantarovich*, I. B. Kevdina*, N. F. Miron*, Yu. V. Baronova, S. S. Berdonosov**, S. B. Baronov**, and I. V. Melikhov****

** Semenov Institute of Chemical Physics, Russian Academy of Sciences, ul. Kosygina 4, Moscow, 119991 Russia*

*** Moscow State University, Moscow, 119992 Russia*

e-mail: berd@radio.chem.msu.ru

Received July 8, 2004

Abstract—Positron annihilation lifetime spectroscopy (PALS) is used to investigate the detailed structure of amorphous alumina tubes prepared via thermohydrolysis of anhydrous $AlCl_3$. The results demonstrate that PALS is a sensitive probe of the structure of amorphous materials, capable of distinguishing between the structures of amorphous alumina tubes and amorphous alumina prepared by a standard procedure, which are shown to differ slightly in the concentration and size of free-volume elements. The observed distinctions can be understood in terms of the anisotropic aggregation of primary alumina particles during hydrolysis in aqueous media or thermohydrolysis in water vapor.

INTRODUCTION

The purpose of this work was to evaluate the average size of free-volume elements (FVEs) in amorphous materials using positron annihilation lifetime spectroscopy (PALS). This method was used earlier in many studies to probe the defect structure of solids [1–6], in particular that of metal oxides, including alumina [7–9].

In PALS, the sample to be studied is irradiated with positrons, and analysis of positron annihilation characteristics provides information about the structure of the material. The annihilation of positrons (via interaction with electrons) in solids may be preceded by several processes, including the formation of positronium Ps, a hydrogen-like system. Owing to exchange interaction, positronium is repelled from host atoms and has time to localize in FVEs of the material (in lattice defects, pores of amorphous materials, and intercrystalline spaces). It is well known that positronium may exist in two forms: long-lived orthopositronium (^{t}Ps) and short-lived parapositronium (^{p}Ps).

The orthopositronium annihilation radiation is more informative in studies of FVEs since the relatively long lifetime of ^{t}Ps depends on the effective size of FVEs in which it is localized. In some cases, the intensity of the long-lived orthopositronium component in the PALS spectrum may depend on the size and concentration of FVEs in the material. The intrinsic lifetime of parapositronium is much shorter (1.25×10^{-10} s), and ^{p}Ps annihilation is not very informative.

Taking into account the processes preceding ^{t}Ps annihilation and using application programs, one can distinguish PALS components differing in lifetime τ_i and intensity I_i. Two components are due to singlet positronium and free positron annihilation. The third component and, occasionally, the fourth and fifth components are due to orthopositronium annihilation and carry information about the FVEs in the material.

Most PALS studies of metal oxides were carried out in the 1970s. In recent years, considerable research effort has been concentrated on nanoparticulate amorphous oxide materials. In this context, it is of interest to assess the potentialities of PALS in probing the fine structure of such systems.

In this work, we focus on amorphous alumina tubes. It has been shown very recently [10–13] that the thermohydrolysis (150–230°C) of anhydrous aluminum chloride yields alumina tubes 80–100 μm to 3–7 cm in length and 20 to 300 μm in diameter (Fig. 1) owing to the self-organization of primary particles. The process is run in a heated reactor. Anhydrous $AlCl_3$ is spread over an inert material (e.g., in a porcelain boat). The surface layer of aluminum chloride is first partially hydrolyzed by exposing the sample to water vapor. Next, the sample is heated in a gas stream (hydrogen, helium, air, or CO_2), which leads to rapid (up to 0.5 mm/s) growth of tubes.

As shown by x-ray fluorescence analysis and radiotracer measurements, the x-ray amorphous tubes thus prepared consist mainly of oxygen and aluminum, with 3.9–4.3 at % Cl impurity. According to ^{27}Al NMR results, the Al atoms in the tubes are in octahedral oxygen coordination, in contrast to conventional amorphous alumina, in which Al atoms are in tetrahedral or mixed (tetrahedral + octahedral) coordination.

0020-1685/05/4103-0255 © 2005 Pleiades Publishing, Inc.

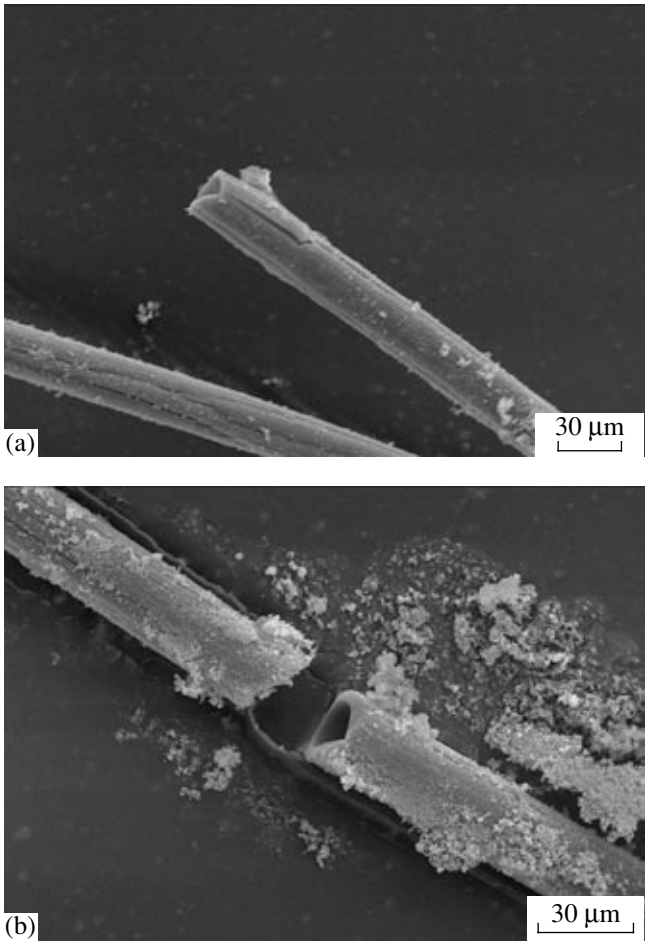

Fig. 1. SEM micrographs of alumina tubes.

Scanning electron microscopy (SEM) examination demonstrates that the tubes consist of particles 150 to 200 nm in size (in accordance with nitrogen BET surface area measurements), firmly bonded to each other. Such particles are assumed to be composed of primary particles 5 to 40 nm in size [12, 13]. It is of interest to use PALS in order to gain further insight into the structure of the tubes and the processes underlying their formation. Note that systematic comparative PALS studies of amorphous and crystalline Al_2O_3 materials have not yet been reported.

In this work, PALS was used to characterize FVEs in amorphous Al_2O_3 and, for comparison, in aluminum hydroxide (intermediate product of $AlCl_3$ thermohydrolysis), thermohydrolysis by-products, and polycrystalline α-Al_2O_3 (corundum).

EXPERIMENTAL

Sample preparation and characterization. To prepare tubular particles, anhydrous $AlCl_3$ (2 g) was spread over a porcelain boat and exposed for 3–4 h to humid air. Next, the sample was heated to 220–250°C in a gas flow. The forming tubes were withdrawn from the boat with forceps and were then stored in a vial at room temperature. The residual powder was also withdrawn from the boat for characterization.

Amorphous alumina was prepared by a standard procedure, by dehydrating aluminum hydroxide [14]. The starting solution (10% $AlCl_3$) was cooled to 0°C, and 25% aqueous ammonia, also cooled to 0°C, was added. The resulting precipitate was collected on a filter and washed with water to neutral pH. Next, it was placed in a porcelain dish and dried in a desiccator over P_2O_5 for 2 weeks. α-Al_2O_3 (corundum) was prepared by calcining aluminum hydroxide at 900°C for 4 h.

All of the samples were characterized by SEM and x-ray diffraction (XRD).

Positron annihilation studies. PALS spectra were measured on a standard EGG&ORTEC fast–fast spectrometer (pulse height analysis in the fast channel). The time resolution (full width at half maximum of the instant-coincidence curve) was 250 ps. As the positron source, we used Ni-sheathed $^{22}NaCl$. The PALS spectrum was stored in a multichannel analyzer (1024 40-ps channels). The total statistics (net count) was above several times 10^6 coincidences. The spectra were analyzed using the POSITRONFIT code, which takes into account the chance coincidence background, resolution fluctuations, and annihilation in the source material.

The PALS spectra of the samples studied are shown in Fig. 2. The lifetimes τ_i and intensities I_i extracted from these spectra are listed in Table 1. Analysis of these data indicates that the components τ_3 (I_3) and τ_4 (I_4) arise from orthopositronium annihilation in FVEs and, hence, can be used to evaluate their parameters.

The effective FVE radius was determined using the Tao–Eldrup–Jean semiempirical formula [2, 3], corrected (which makes sense at positronium lifetimes over 10 ns) for the intrinsic lifetime of orthopositronium, $\tau_0^t = (\lambda_0^t)^{-1}$ [9]:

$$\lambda_i = \frac{1}{\tau_i} = \lambda_0^t + 2\left[1 - \frac{R_i}{R_i + \Delta R} + \frac{1}{2\pi}\sin\left(\frac{2\pi R}{R_i + \Delta R}\right)\right] \text{ns}^{-1}. \quad (1)$$

For components 3 and 4, $i = 3$ and 4, respectively.

ΔR, which characterizes the penetration of positronium into FVEs, was taken to be 0.166 nm [2, 3] based on calibration results for different substances.

In determining the FVE concentration, we took into account that an orthopositronium atom may appear in an FVE (pore) as a result of several processes, of which the following are the most important:

I. A positronium atom forms, with probability Q, in the material being studied and then diffuses until it is captured by an FVE. Further, two situations are possi-

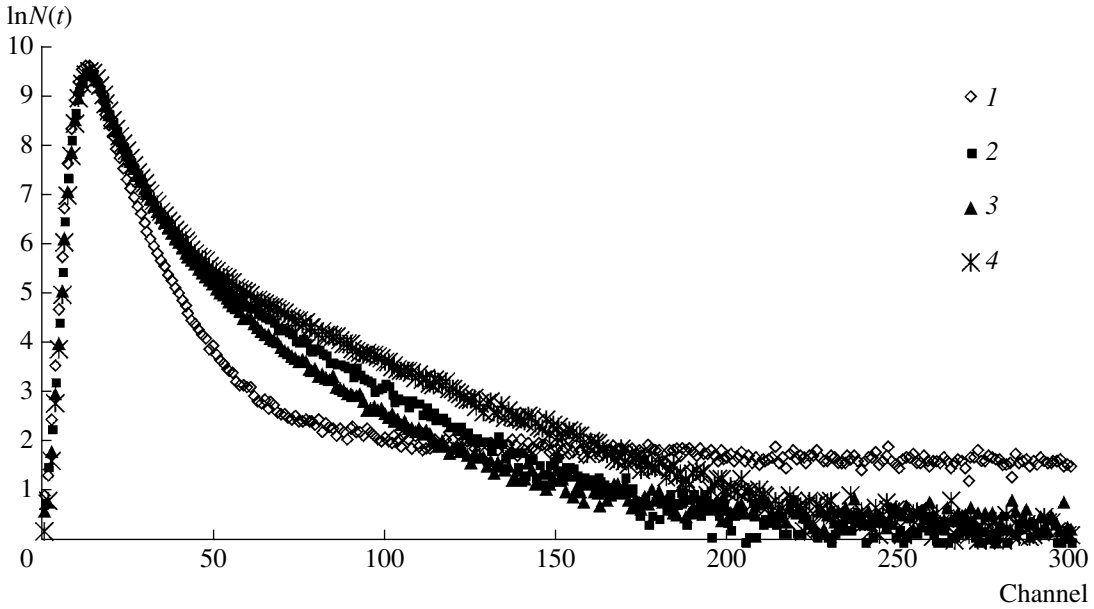

Fig. 2. PALS spectra of (*1*) α-Al_2O_3 (corundum), (*2*) amorphous Al_2O_3 tubes, (*3*) thermohydrolysis by-products, and (*4*) amorphous Al_2O_3.

ble. (Ia) If the annihilation rate of free (nonlocalized) positronium is comparable to the capture rate, these processes compete with one another. An important point is that the amount of orthopositronium (the intensities of the long-lived components I_3 and I_4) is determined by the FVE concentration, which can, therefore, be inferred from the annihilation characteristics. (Ib) If the FVE concentration is so high that the positron capture rate far exceeds the rate of positron annihilation, I_3 and I_4 are determined not by the FVE concentration but by the probability Q of positronium formation in the material. In this case, the FVE concentration cannot be evaluated from PALS data.

II. Positronium forms in a free volume after a positron has found its way into it. The rate of positronium formation is then limited by the FVE concentration (and possibly by the electron density in the track).

Thus, in processes I and II, the precursors to localized positronium are a nonlocalized positronium atom and a positron, respectively.

Processes I and II are described by similar rate equations of the form (2) [4, 5], which take into account

Table 1. Annihilation characteristics of Al_2O_3 samples

Sample	$Al(OH)_3$	Amorphous alumina tubes	Amorphous alumina	Amorphous by-product	α-Al_2O_3 (corundum)
τ_1, ns	0.2562 ± 0.0044	0.2793 ± 0.0039	0.2853 ± 0.0033	0.2753 ± 0.0039	0.1967 ± 0.0017
I_1, %	59.3483 ± 2.3807	69.5131 ± 1.9203	69.9829 ± 1.7346	69.5723 ± 2.4763	72.7119 ± 1.0166
τ_2, ns	0.5245 ± 0.0215	0.6434 ± 0.0392	0.6223 ± 0.0338	0.5805 ± 0.0436	0.4273 ± 0.0078
I_2, %	27.087 ± 2.126	20.5043 ± 1.3435	16.8671 ± 1.4716	21.7022 ± 1.4573	22.4938 ± 1.0365
τ_3, ns	1.6811 ± 0.0283	1.4737 ± 0.0338	1.7614 ± 0.0171	1.2109 ± 0.0573	2.5205 ± 0.3697
I_3, %	10.161 ± 0.357	9.9827 ± 0.8173	13.1500 ± 0.3611	8.3491 ± 1.3894	0.5890 ± 0.0434
τ_4, ns	35.0336 ± 1.6429		–	9.6733 ± 0.8037	42.3578 ± 4.7024
I_4, %	3.404 ± 0.076		–	0.3764 ± 0.0185	4.2054 ± 0.2415

either the behavior of the positrons ($k = e^+$) forming orthopositronium upon localization or the behavior of orthopositronium ($k = Ps$) localizing in a free volume,

$$\begin{cases} dP_f^k/dt = -\lambda_f P_f^k - \sum_i \nu_i P_f^k, \\ dP_i^k/dt = (3/4)\nu_i P_f^k - \gamma_i P_i^k, \end{cases} \quad (2)$$

with boundary conditions $P_f^k(0) = 1$ at $k = e^+$ and $P_f^k(0) = Q$ at $k = Ps$. Here, P_i and P_f are the probabilities of finding a precursor to localized orthopositronium in a localized microvolume of type i or in a free state (subscript f). The factor 3/4 appears because we consider annihilation of triplet positronium. The parameter Q represents the fraction of positrons involved in positronium formation.

Occasionally, annihilation spectra showed two positronium components, indicating that the sample contained two types of free volumes. The following equations, relating the positron capture rates ν_3 and ν_4 to annihilation characteristics, were obtained for two types of free volumes:

$$\nu_3 = \frac{I_3}{A}\left[(\lambda_f - \gamma_3)\left(\frac{3}{4}Q - I_4\right) + (\lambda_f - \gamma_4)I_4\right],$$

$$\nu_4 = \frac{I_4}{A}\left[(\lambda_f - \gamma_4)\left(\frac{3}{4}Q - I_3\right) + (\lambda_f - \gamma_3)I_3\right], \quad (3)$$

$$A = \left(\frac{3}{4}Q - I_3\right)\left(\frac{3}{4}Q - I_4\right) - I_3 I_4.$$

If there is only one type of defect, Eqs. (3) take the form

$$\nu_3 = (4/3)I_3\frac{\lambda_f - \gamma_3}{Q - (4/3)I_3}, \quad (4)$$

where λ_f is the annihilation rate of free (nonlocalized) positrons (positronium) and $\gamma_i = 1/\tau_i$. Process II corresponds to $Q = 1$. For situation Ia, we take, as a rough approximation, $Q = 1 - I_2$ (nonlocalized positronium is assumed to make an insignificant contribution to this component).

In the cases under consideration, the relationship between the capture rates ν_i and the FVE concentration is of importance. For the capture of nonlocalized positronium (Ia), we have

$$N_i = \frac{\nu_i}{4\pi D^{Ps} R_i}, \quad (5)$$

for the capture of a nonlocalized positron (II),

$$N_i = \frac{\nu_i}{4\pi D^{+} R_i}, \quad (6)$$

where D^+ and D^{Ps} are the respective diffusion coefficients. It is commonly believed that, at least in amorphous materials, these coefficients differ substantially: $D^+ \simeq 10^{-3}$ to 10^{-1} cm^2/s [15, 16] and $D^{Ps} = 10^{-5}$ to 10^{-4} cm^2/s [9, 17, 18]. For this reason, the concentrations estimated for different cases may differ markedly.

RESULTS AND DISCUSSION

The annihilation characteristics of Al_2O_3 tubes and conventional amorphous Al_2O_3 are listed in Table 1 in comparison with those of references samples. A few features of these data warrant attention.

1. The spectra of tubular and amorphous Al_2O_3 show only one positronium component (τ_3, I_3), with a relatively short lifetime of 1.47–1.76 nm.

2. The spectrum of α-Al_2O_3 shows two orthopositronium components (τ_3, I_3 and τ_4, I_4), but the intensity of the former is very low, which is attributable to crystallization of amorphous microparticles.

3. According to earlier results [12, 13], the minimum particle size of amorphous Al_2O_3 does not exceed 100 nm. This value is very close to the diffusion length of positrons in solids, $\lambda^+ = \sqrt{6D\tau}$, at $D^+ = 0.001$–0.1 cm^2/s [15, 17] and $\tau = 0.2$–0.3 ns and far exceeds the diffusion length of nonlocalized positronium at $D^{Ps} \simeq 10^{-5}$ to 10^{-4} cm^2/s [15, 17] and the same τ [4, 17, 18].

In going from amorphous Al_2O_3 microparticles to microcrystalline corundum, the short-lived positronium component (τ_3, I_3) essentially disappears ($I_3 \simeq 0.4\%$). It is, therefore, reasonable to assume that this component, present in amorphous microparticles, is due to internal microvolumes (to the presence of FVEs, which are very few and far between in the microcrystallites). Since the long-lived component τ_4, attributable to interparticle free volumes, is missing in amorphous Al_2O_3, we conclude that positronium does not reach the interparticle regions. At the same time, as pointed out by Bartenev *et al.* [7], some of the particles in question are no greater than hundreds of nanometers in size, and, in view of the large diffusion coefficient, $D^+ = 0.1$ cm^2/s, a positron might reach the microparticle surface and form positronium (mechanism II). Since this is not the case, we are led to assume that positronium is formed in the bulk of amorphous grains (this is possible if the diffusion coefficient of nonlocalized positronium is $D^{Ps} = 10^{-5}$ to 10^{-4} cm^2/s [4, 17–19]).

Thus, it seems likely that mechanism Ia prevails. Therefore, the FVE concentration in microparticles can be evaluated by Eq. (4). For definiteness, we take $D^{Ps} = 10^{-4}$ cm^2/s. The estimated FVE concentrations in amorphous tubes and conventional amorphous Al_2O_3 are listed in Table 2.

It is clear from Table 2 that, even though the amorphous materials are rather close in N_3 and R_3, they

Table 2. Average radius R and concentration N of FVEs in amorphous and crystalline aluminas

Material	Amorphous Al_2O_3	Amorphous Al_2O_3 tubes	α-Al_2O_3
R_3, nm	0.263	0.23	0.33
N_3, cm^{-3}	12.437×10^{19}	9.68×10^{19}	0.568×10^{16}
R_4, nm	–	–	1.34
N_4, cm^{-3}	–	–	1.138×10^{16}

have a number of marked distinctions, which are probably associated with the fact that the materials prepared by vapor-phase hydrolysis and vapor-phase topochemical processes differ in structural parameters [12].

In the case of α-Al_2O_3, the long-lived component with $\tau_4 > 40$ ns, usually missing in molecular crystals, warrants attention. It seems likely that this component arises from the annihilation of the positronium formed at crystallite boundaries. This mechanism was discussed repeatedly in the literature [9, 20, 21]. Moreover, the positronium mobility in crystalline phases is rather high [22]. Since positrons (positronium) may appear in intercrystalline free volumes, the parameters of component τ_4 (I_4) must depend on the particle size of the material, as pointed out in earlier studies of metal oxides [7]. This effect may be significant at crystallite sizes below several hundred nanometers.

Thus, using PALS results and Eq. (5), and taking $D^+ = 0.1$ cm^2/s, one can estimate the concentration N_4 and effective size R_4 of intercrystalline regions. Similar reasoning applies to the low concentration N_3 of intercrystalline defects, which are responsible for the weak component τ_3 (I_3). The results for this component are also presented in Table 2.

Note that component τ_4 (I_4) is also prominent in the spectrum of aluminum hydroxide (Table 1). The microstructural features of the hydroxide responsible for this component may influence the size of α-Al_2O_3 microcrystallites prepared by calcining the hydroxide at 900°C for 4 h.

Component τ_4, though very weak (0.37%), also appears in the spectrum of the residual powder. Presumably, this component is due to a small (about 10%) fraction of oxide crystallites or hydroxide microparticles that were formed during $AlCl_3$ thermohydrolysis.

CONCLUSIONS

Our results demonstrate that PALS makes it possible to reveal fine details of the structure of amorphous alumina, in particular to distinguish between the structures of fine-particle amorphous alumina and amorphous tubes. At the same time, the annihilation characteristics of these materials differ not very strongly, indicating that they are similar in structure.

Comparison of the PALS data for α-Al_2O_3 (corundum), amorphous alumina, and alumina tubes provides some insight into the mechanism of positron annihilation in alumina tubes and allows one to evaluate the concentration (about 10^{20} cm^{-3}) and effective radius ($R_3 \simeq 2.3$ Å) of FVEs in the material.

Remarkably, we were able to reveal a very slight difference in the concentration and effective size of FVEs between alumina tubes and conventional amorphous alumina, which seems to be related to the difference in the preparation procedure.

ACKNOWLEDGMENTS

This work was supported by the Russian Foundation for Basic Research (grant nos. 03-02-32061 and 03-03-32918) and the President's Grants Council for Support to Leading Scientific Schools (grant no. NSh-1818-2003.3).

REFERENCES

1. Melikhov, I.V., Shantarovich, I.P., Kitova, E.N., *et al.*, Microscopic Radionuclidic Characterization of Disperse Solid Phases, *Zh. Fiz. Khim.*, 1993, vol. 67, no. 1, pp. 75–79.
2. Tao, S.J., Positronium Annihilation in Molecular Substances, *J. Chem. Phys.*, 1972, vol. 56, no. 11, p. 5499.
3. Eldrup, M., Lightbody, D., and Sherwood, L.N., The Temperature Dependence of Positron Life Times in Solid Pivalic Acid, *Chem. Phys.*, 1981, vol. 36, no. 1, p. 51.
4. Shantarovich, V.P. and Goldanskii, V.I., On the Role of Free Volume in Positron Annihilation in Polymer Structures, *Hyperfine Interact.*, 1998, vol. 116, no. 1, p. 67.
5. Shantarovich, V.P., Suzuki, T., He, C., *et al.*, Positron Annihilation Study of Hyper-Cross-Linked Polystyrene Networks, *Macromolecules*, 2002, vol. 35, no. 26, p. 9723.
6. Shantarovich, V.P., Gustov, V.V., Kevdina, I.B., *et al.*, Study of Structural Defects in $CaSO_4 \cdot 2H_2O$ Crystals by Positron Annihilation and Radiothermoluminescence, *Neorg. Mater.*, 1997, vol. 33, no. 8, pp. 1007–1011 [*Inorg. Mater.* (Engl. Transl.), vol. 33, no. 8, pp. 853–856].
7. Bartenev, G.M., Varisov, A.Z., Goldanskii, V.I., *et al.*, Particle Size Effect on Positron Annihilation in Some Metal Oxides, *Fiz. Tverd. Tela* (Leningrad), 1969, vol. 11, no. 11, p. 3177.
8. Paulin, R. and Ambrosino, J., Free Annihilation of the Ortho-positronium Formed in Some Powders with a High Specific Surface, *J. Phys.* (Paris), 1968, vol. 29, no. 2, p. 263.
9. Kusmiss, J.H and Stewart, A.T, Positron Annihilation in Solid and Liquid Metals, *Positron Annihilation,* Stewart, A.T. and Roellig, L.O., Eds., New York: Academic, 1967, p. 341.

10. Berdonosov, S.S., Baronov, S.B., Kuz'micheva, Yu.V., *et al.*, Hollow Alumina Macrotubes, *Neorg. Mater.*, 2001, vol. 37, no. 10, pp. 1219–1223 [*Inorg. Mater.* (Engl. Transl.), vol. 37, no. 10, pp. 1037–1040].
11. Berdonosov, S.S., Baronov, S.B., Kuz'micheva, Yu.V., *et al.*, Hollow Macrotubes: A New, Elegantly Textured Form of Amorphous Alumina, *Vestn. Mosk. Univ., Ser. 2: Khim.*, 2002, vol. 43, no. 1, pp. 64–67.
12. Berdonosov, S.S., Melikhov, I.V., Baronov, S.B., *et al.*, Thermohydrolysis Route to Tubular Alumina, *Dokl. Akad. Nauk*, 2002, vol. 383, no. 2, pp. 211–214.
13. Baronov, S.B., Berdonosov, S.S., Kuz'micheva, Yu.V., and Melikhov, I.V., Self-organization of Alumina: From Nanoparticles to Tubular Forms, *Izv. Akad. Nauk, Ser. Fiz.*, 2003, vol. 67, no. 7, pp. 912–914.
14. *Handbuch der präparativen anorganischen Chemie in drei Bänden*, von Brauer, G., Ed., Stuttgart: Ferdinand Enke, 1978, 3rd ed. Translated under the title *Rukovodstvo po neorganicheskomu sintezu v 6 tomakh,* Moscow: Mir, 1985, vol. 3.
15. Nieminen, R.M and Manninen, M.J, Positron in Imperfect Solids: Theory, *Positron in Solids*, Hautojarvi, P., Ed., Berlin: Springer, 1979, p. 148.
16. Weber, M.H and Lynn, K.G, Positron Porosimetry, *Positron and Positronium Chemistry*, Jean, Y.C. *et al.*, eds., New York: World Scientific, 2003, p. 174.
17. Waran, K.V., Cheng, K.L., and Jean, Y.C., Application of Positron Annihilation To Study the Surface Properties of Porous Resins, *J. Phys. Chem.*, 1984, vol. 88, no. 12, p. 2465.
18. Shantarovich, V.P., Novikov, Yu.A., and Azamatova, Z.K., Positron Annihilation Study of Free Volume Elements in Polymeric Gas-Separation Membranes, *Fiz. Tverd. Tela* (S.-Peterburg), 1998, vol. 40, no. 1, pp. 164–167.
19. Brandt, W. and Paulin, R., Positron Diffusion in Solids, *Phys. Rev. Lett.*, 1968, vol. 21, p. 193.
20. Perkal, M.B. and Walters, W.B., Positron Annihilation in Synthetic Zeolites 4A and 13X, *J. Chem. Phys.,* 1970, vol. 53, no. 1, pp. 190–198.
21. Goldanskii, V.I., Mokrushin, A.D., Tatur, A.O., and Shantarovich, V.P., Positronium–Gas Interaction in Pores of Silica Gel, *Kinet. Katal.*, 1972, vol. 13, no. 4, p. 961.
22. Greenberger, A., Mills, A.P., Thompson, A., and Berko, S., Evidence for Positron-like Bloch States in Quartz Single Crystals, *Phys. Rev. Lett.*, 1970, vol. 32A, no. 1, p. 72.